Accurate formula for dissipative interaction in frequency modulation atomic force microscopy

Kazuhiro Suzuki,[1] Kei Kobayashi,[1,2] Aleksander Labuda,[3] Kazumi Matsushige,[1] and Hirofumi Yamada[1]

[1]*Department of Electronic Science and Engineering, Kyoto University, Katsura, Nishikyo, Kyoto 615-8510, Japan*

[2]*The Hakubi Center for Advanced Research, Kyoto University, Katsura, Nishikyo, Kyoto 615-8520, Japan*

[3]*Department of Physics, McGill University, Montreal H3A 2T8, Canada*

(Received 25 August 2014; accepted 23 November 2014; published online 8 December 2014)

Much interest has recently focused on the viscosity of nano-confined liquids. Frequency modulation atomic force microscopy (FM-AFM) is a powerful technique that can detect variations in the conservative and dissipative forces between a nanometer-scale tip and a sample surface. We now present an accurate formula to convert the dissipation power of the cantilever measured during the experiment to damping of the tip-sample system. We demonstrated the conversion of the dissipation power versus tip-sample separation curve measured using a colloidal probe cantilever on a mica surface in water to the damping curve, which showed a good agreement with the theoretical curve. Moreover, we obtained the damping curve from the dissipation power curve measured on the hydration layers on the mica surface using a nanometer-scale tip, demonstrating that the formula allows us to quantitatively measure the viscosity of a nano-confined liquid using FM-AFM. © *2014 AIP Publishing LLC*. [http://dx.doi.org/10.1063/1.4903484]

Much attention has recently been paid to nano-confined liquids by researchers in various fields such as biophysics, tribology, geophysics and nanotechnology.[1–4] The viscosity of a nano-confined liquid has been intensively studied using surface force apparatus (SFA) technique and atomic force microscopy (AFM).[5–8] In particular, frequency-modulation AFM (FM-AFM) in liquids, an emerging technique that allows us to measure the interaction forces in a three-dimensional (3D) volume near the solid/liquid interface with a molecular resolution,[9–12] is a promising tool for investigation of the viscosity of a nano-confined liquid with a high spatial resolution. We recently demonstrated that 3D force maps obtained by FM-AFM at the mica/water interface reflect the structured water layers on the mica surface.[10–12] In these experiments, the hydration force exerted on the tip at the end of a cantilever was measured as the resonance frequency shift of the cantilever. The frequency shift measured during the experiment was subsequently converted to the conservative interaction force and energy using analytical equations.[13,14] One of the great advantages of FM-AFM is that the conservative and dissipative interaction forces can be simultaneously and independently measured. During the FM-AFM experiments, the oscillation amplitude of the cantilever is usually kept constant (constant amplitude mode). If the dissipative interaction force is exerted on the tip, an additional input power is required to keep the oscillation amplitude constant; otherwise, the oscillation stops; the magnitude of the additional input power is a measure of the dissipation power in the tip-sample system. If the dissipation power of the cantilever can be converted to the damping coefficient of the system, FM-AFM can be used to quantitatively measure the viscosity of a nano-confined liquid with a high sensitivity as well as a high spatial resolution since the relationship between the damping and viscosity has been well established.[15] However, the dissipation power of the cantilever is measured as an average value over an oscillation cycle, in which the tip travels back and forth for a distance on the order of nanometers in the medium having a local variation in the viscosity, therefore, the conversion of the dissipation power to the damping or the viscosity is not straightforward. Although several researchers have published papers on the methods to convert the dissipation power to the damping or viscosity, they were analytical formulas which were only valid for cases in which the oscillation amplitude is far smaller or larger than the characteristic length of the local variation in the damping or viscosity,[16,17] otherwise one had to convert the dissipation power to the damping using a computer simulation.[18] An analytical formula to convert the dissipation power to the damping coefficient of the system regardless of the oscillation amplitude of the cantilever has not yet been established.

In this study, we derive an accurate formula to convert the dissipation power of the cantilever to the damping regardless of the oscillation amplitude. We first applied the equation to convert the dissipation power versus separation curve obtained by FM-AFM with a colloidal probe at a mica-solution interface. Then, the dissipation power was recovered from the damping curve to confirm the validity of the formula. Second, we more accurately converted the dissipation power curve for the hydration layers on the mica surface using a nanometer-scale tip to the damping coefficient than previously reported,[12] thus showing the variation in the viscosity in the hydration layers.

The equation of motion of an oscillated cantilever in dynamic-mode AFM is expressed as

$$m\frac{d^2q(t)}{dt^2} + \gamma(z + A + q(t))\frac{dq(t)}{dt} + kq(t) - F_{\mathrm{int}}(z + A + q(t)) = F_{\mathrm{d}}(z, t), \quad (1)$$

where q is displacement of the cantilever, t is the time, m is the effective mass of the cantilever, $\gamma(z)$ is the damping, z is the closest tip-sample distance during an oscillation cycle, k is the spring constant of the cantilever, F_{int} is the conservative interaction force acting on the tip, A is the oscillation amplitude, and $F_{\mathrm{d}}(z,t)$ on the right side represents the drive force. $\gamma(z)$ can be expressed as $\gamma(z) = \gamma_0 + \gamma_{\mathrm{tip}}(z)$, where $\gamma_{\mathrm{tip}}(z)$ is the damping of the tip-sample system on which we will focus. γ_0 is a parameter corresponding to the intrinsic damping of the cantilever that is constant throughout the experiment, which is defined as $k/(Q\omega_0)$, where Q and ω_0 are the mechanical quality factor and natural angular resonance frequency, respectively.

The dissipation power in the tip-sample system (P_{tip}) caused by the dissipative interaction force acting on the tip is calculated as the balance between the input power to the system (P_{input}) and the dissipation power in the cantilever-sample system ($P_{\mathrm{cantilever}}$). P_{input} and $P_{\mathrm{cantilever}}$ are calculated from the right and left sides of Eq. (1), respectively, as

$$P_{\mathrm{input}} = \frac{\omega(z)}{2\pi}\oint F_{\mathrm{d}}(z,t)dq \tag{2}$$

and

$$P_{\mathrm{dissipation}} = \frac{\omega(z)}{2\pi}\oint\left[\gamma_0 + \gamma_{\mathrm{tip}}(z+A+q(t))\right]\frac{dq(t)}{dt}dq. \tag{3}$$

For the FM-AFM in the constant amplitude mode, the difference between the phases of $q(t)$ and $F_{\mathrm{d}}(z,t)$ is maintained at $\pi/2$ by a self-oscillation loop or a phase-locked loop, and A remains constant by an automatic gain controller during the experiment. Therefore, we write $q(t)$ and $F_{\mathrm{d}}(z,t)$ as $q(t) = A\cos[\omega(z)t]$ and $F_{\mathrm{d}}(z,t) = -kA_{\mathrm{d}}(z)\sin[\omega(z)t]$, respectively, where A_{d} is the drive amplitude of the cantilever, and obtain

$$P_{\mathrm{input}} = \frac{A\omega(z)}{2}kA_{\mathrm{d}}(z) \tag{4}$$

and

$$P_{\mathrm{dissipation}} = \frac{A^2[\omega(z)]^2}{2}\gamma_0 - \frac{A[\omega(z)]^2}{2\pi} \times \oint\left[\gamma_{\mathrm{tip}}(z+A+q(t))\right]\sin[\omega(z)t]dq. \tag{5}$$

The first and second terms in Eq. (5) represent the dissipation power in the cantilever-sample system (P_0) and that in the tip-sample system (P_{tip}). Therefore, P_{tip} is calculated from the experimental parameters as[16]

$$P_{\mathrm{tip}}(z) = \frac{A\omega(z)}{2}kA_{\mathrm{d}}(z) - \frac{A^2[\omega(z)]^2}{2}\gamma_0 = \frac{A^2[\omega(z)]^2}{2}\gamma_0\left(\frac{\omega_0 A_{\mathrm{d}}(z)}{\omega(z)A_{\mathrm{d0}}} - 1\right), \tag{6}$$

where A_{d0} is the drive amplitude at the start of the experiment defined as A/Q.

To obtain $\gamma_{\mathrm{tip}}(z)$ from the experimental data, one has to invert the relationship

$$P_{\mathrm{tip}}(z) = -\frac{A[\omega(z)]^2}{2\pi}\oint\left[\gamma_{\mathrm{tip}}(z+A+q(t))\right]\sin[\omega(z)t]dq. \tag{7}$$

For the cases when the oscillation amplitude is significantly smaller than the characteristic length of the variation in the damping, $\gamma_{\mathrm{tip}}(z)$ is considered to be constant for the tip travel range during an oscillation cycle. Therefore, $\gamma_{\mathrm{tip}}(z)$ can be obtained from the experimental parameters using Eq. (6) as

$$\gamma_{\mathrm{tip}}(z) = \frac{2}{A^2[\omega(z)]^2}P_{\mathrm{tip}}(z) = \gamma_0\left(\frac{A_{\mathrm{d}}(z)}{A_{\mathrm{d0}}}\frac{\omega_0}{\omega(z)} - 1\right). \tag{8}$$

On the other hand, for the case when the oscillation amplitude is far greater than the characteristic length of the variation in the damping, the analytical formula presented by Dürig can be used to calculate $\gamma_{\mathrm{tip}}(z)$.[17] Except for such extreme cases, $\gamma_{\mathrm{tip}}(z)$ had only been accessible by a computational simulation as already mentioned.[18]

In the following text, we present an analytical formula for calculating $\gamma_{\mathrm{tip}}(z)$ from the measured parameters, derived in the same way as those for calculating the conservative force from the frequency shift[14] and the instantaneous tunneling current from the time-averaged tunneling current.[19] Equation (7) can be expressed as

$$P_{\mathrm{tip}}(z) = \frac{A^2[\omega(z)]^2}{\pi}\int_{-1}^{1}\gamma_{\mathrm{tip}}(z+A(1+u))\sqrt{1-u^2}\mathrm{d}u \tag{9}$$

with $u = q(t)/A = \cos[\omega(z)t]$. Equation (9) is similar to those for the frequency shift and the conservative force and[14] and for the time-averaged tunneling current and the instantaneous tunneling current.[19] The weight function $\sqrt{1-u^2}$ in the integrand is different from those; $u/\sqrt{1-u^2}$ for the conservative force[14] and $1/\sqrt{1-u^2}$ for the tunneling current.[19]

First, γ_{tip} is converted to an integral representation

$$\gamma_{\mathrm{tip}}(z) = \int_0^\infty B(\lambda)\exp(-\lambda z)d\lambda, \tag{10}$$

which is the Laplace transform of $B(\lambda)$. $P_{\mathrm{tip}}(z)$ then becomes

$$P_{\mathrm{tip}}(z) = A^2[\omega(z)]^2\int_0^\infty B(\lambda)\frac{T(\lambda A)}{\lambda A}\exp(-\lambda z)d\lambda, \tag{11}$$

where $T(y) = I_1(y)\exp(-y)$, and $I_1(y)$ is the first order modified Bessel function of the first kind. The Laplace transform and the inverse Laplace transform are now expressed as $L\{\}$ and $L^{-1}\{\}$, respectively, and the damping coefficient γ_{tip} becomes

$$\gamma_{\mathrm{tip}}(z) = L\left\{\frac{\lambda A}{T(\lambda A)}L^{-1}\left\{\frac{P_{\mathrm{tip}}(z)}{A^2\omega(z)^2}\right\}\right\}. \tag{12}$$

In order to analytically calculate Eq. (12), the Pade approximation for $T(y)$, which is

$$T(y) = \frac{y}{2}\left(1 + \frac{1}{8}\sqrt{y} + \sqrt{\frac{\pi}{2}}y^{3/2}\right)^{-1} \tag{13}$$

is used.[14] The maximum error of this approximation is within 5%. Finally, taking advantage of the properties of the

Riemann-Liouville fractional integral,[14] the following equation is obtained:

$$\gamma_{\mathrm{tip}}(z) = \frac{2P_{\mathrm{tip}}(z)}{A^2[\omega(z)]^2} - \frac{1}{4\sqrt{\pi}A^{3/2}}\int_z^\infty \frac{1}{\sqrt{\tau - z}}\frac{d}{d\tau} \times \left(\frac{P_{\mathrm{tip}}(\tau)}{[\omega(\tau)]^2}\right)d\tau + \sqrt{\frac{2}{A}}\int_z^\infty \frac{1}{\sqrt{\tau - z}}\frac{d^2}{d\tau^2}\left(\frac{P_{\mathrm{tip}}(\tau)}{[\omega(\tau)]^2}\right)d\tau. \quad (14)$$

Note that all three terms on the right side of Eq. (14) have different powers of A as weighting factors. When A is small compared to the range of the dissipative interaction, namely, $A \ll s$, where s is a scaling parameter for the range of the dissipative interaction, the first term on the right side of Eq. (14) is dominant. This term corresponds to Eq. (8). On the other hand, when $A \gg s$, an approximate equation

$$\gamma_{\mathrm{tip}}(z) \approx \sqrt{\frac{2}{A}}\int_z^\infty \frac{1}{\sqrt{\tau - z}}\frac{d^2}{d\tau^2}\left(\frac{P_{\mathrm{tip}}(\tau)}{\omega(\tau)^2}\right)d\tau \quad (15)$$

is obtained, because the third term is much larger than any other terms on the right side of Eq. (14). When the variation in the frequency shift is small enough compared to that in the dissipation power, Eq. (15) is simplified as

$$\gamma_{\mathrm{tip}}(z) \approx \sqrt{\frac{2}{A}}\frac{1}{\omega(z)^2}\int_z^\infty \frac{1}{\sqrt{\tau - z}}\frac{d^2P_{\mathrm{tip}}(\tau)}{d\tau^2}d\tau, \quad (16)$$

which corresponds to the analytical equation derived by Dürig.[17]

To demonstrate the inversion equation presented as Eq. (14), we measured the damping in the tip-sample system using a colloidal probe cantilever. We used a gold-coated colloidal probe cantilever, FmG01_Bio900/Au (NT-MDT), and a cleaved muscovite mica. A SiO_2 colloid whose radius was 450 nm was fixed on the cantilever with a Au backside coating. The nominal spring constant and resonance frequency of the cantilever measured in a 1.0 M KCl aqueous solution were 3 N/m and 23.9 kHz, respectively.

The instrument we used was a modified AFM instrument (Shimadzu SPM-9600) with a home-built controller. The cantilever was oscillated by the photothermal excitation method, which made it possible to quantitatively measure the dissipation power and the frequency shift.[10,12,20]

Figures 1(a) and 1(b) show plots of the frequency shift and normalized drive amplitude ($A_{\mathrm{d}}(z)/A_{\mathrm{d0}}$) as a function of z, which was corrected for the static deflection of the cantilever and thereby referred to as separation hereafter. The curves are shown after the averaging of 128 curves. The oscillation amplitude was kept constant at 9.0 nm peak-to-peak ($A = 4.5$ nm). The long-range negative frequency shift in Fig. 1(a) was caused by the hydrodynamic loading. As the cantilever was brought close to the surface, the added mass effect which decreases the resonance frequency became increasingly prominent.[21,22] See Supplementary Material for further explanation on the frequency shift in Fig. 1(a).[23] We first calculated $P_{\mathrm{tip}}(z)$ from Fig. 1(b) using an equation similar to Eq. (6), but considering the frequency dependence of the cantilever damping. See Ref. 10 for the details. The obtained dissipation power curve is shown in Fig. 1(c).

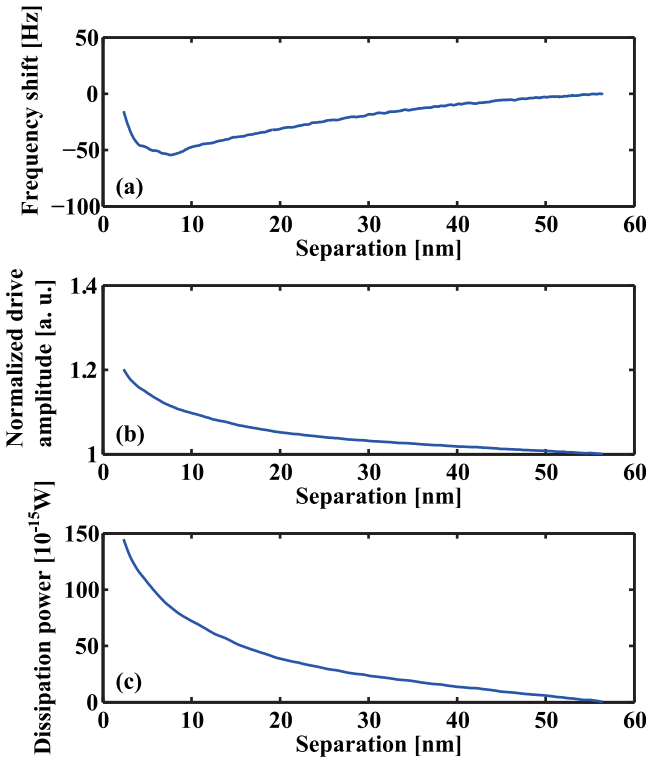

FIG. 1. Frequency shift (a), normalized drive amplitude (b), and dissipation power (c) curves as a function of the tip-sample distance on mica obtained in a 1 M KCl aqueous solution using FM-AFM with a colloidal probe.

Figure 2 shows $\gamma_{\mathrm{tip}}(z)$ calculated from $P_{\mathrm{tip}}(z)$ using Eq. (14). Figure 2(a) shows three parts of $\gamma_{\mathrm{tip}}(z)$, which correspond to the three terms in Eq. (14), among which the first and third terms correspond to the approximated equations for small and large amplitude limits, respectively. When the tip-sample separation was greater than 5 nm, the first term was dominant and gradually increased as the tip was brought closer to the sample surface. This is consistent with the fact that $P_{\mathrm{tip}}(z)$ increased with the characteristic length greater than the oscillation amplitude. On the other hand, when the separation was reduced to less than 4 nm, the contribution of the third term increased.

$\gamma_{\mathrm{tip}}(z)$ obtained as the sum of the three terms plotted in Fig. 2(b) was in good agreement with the theoretical damping curve obtained by

$$\gamma_{\mathrm{tip}}(z) = \frac{6\pi\eta R^2}{z}, \quad (17)$$

where η and R are the viscosity of water (8.9×10^{-4} Pa s) and the radius of the colloid, respectively. Note that the origin of z for the plots in Fig. 1 was determined by the fitting Eq. (17) to Fig. 2(b).

We recovered the dissipation power curve using Eq. (9) to validate the inversion equation, Eq. (14). Figure 2(c) is the dissipation power curve calculated from the experimental damping curve in Fig. 2(b) using Eq. (9), shown together with the original dissipation power curve in Fig. 1(c). They are almost completely overlapped with each other; a slight deviation was possibly due to the error in the approximation used for the computation, Eq. (13). Moreover, we performed a series of the same experiments with different oscillation

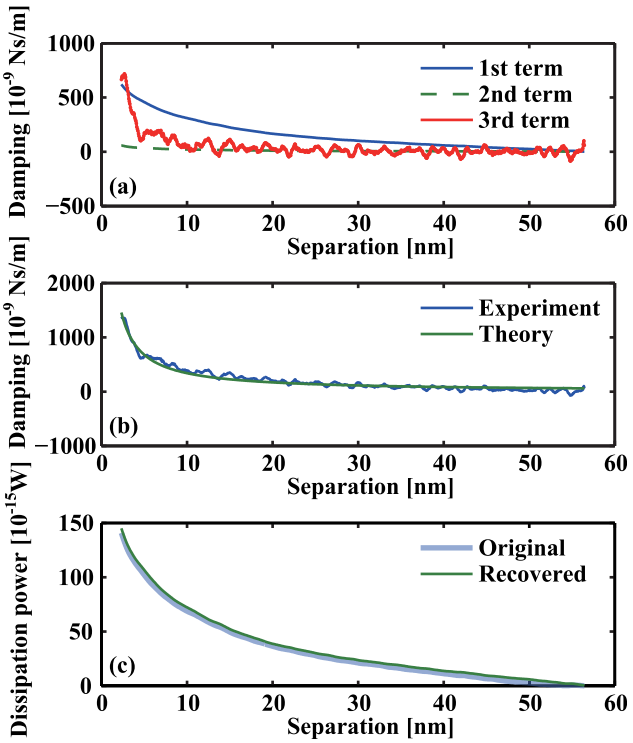

FIG. 2. (a) Damping coefficient terms converted from the dissipation power curve in Fig. 1(c) using Eq. (14). (b) Damping coefficient curve as a function of tip-sample separation as a sum of the three terms in (a). A theoretical curve calculated using Eq. (17) is also shown. (c) Dissipation power curve calculated from the experimental damping curve in (b) using Eq. (9), shown together with the original dissipation power curve in Fig. 1(c).

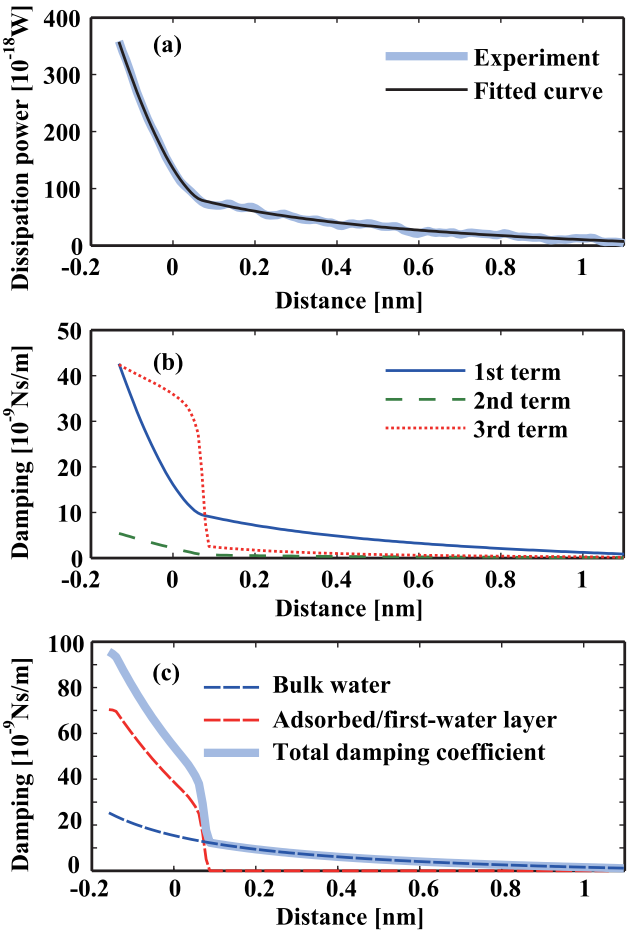

FIG. 3. (a) Dissipation power curve measured at the mica-solution interface and the fitted curve. (b) Converted partial damping curves calculated using the three terms in Eq. (14). (c) Damping coefficient curve converted from the fitted dissipation power curve shown in (a). The damping due to bulk water and the damping due to the adsorbed/first water layer were also plotted.

amplitudes to prove that the inversion equation is valid regardless of the oscillation amplitude.[23] Finally, it is worth to mention here that the inversion formula, Eq. (14), cannot be readily applicable for the dissipation power curve measured in the constant excitation mode. However, the equation could be extended by the same approach taken by Hölscher *et al*. for conversion of the frequency shift curve to the force curve measured in the constant excitation mode.[24]

We next applied Eq. (14) to the dissipation power versus distance curve that we reported as Fig. 3(a) in Ref. 12. Note that the origin of z was defined at the position of the most negative frequency shift.[10,12] We found that the third term in Eq. (14) produces a large fluctuation because it contains a second derivative of the data. As the original experimental data were not sufficiently averaged, we obtained the smooth dissipation power curve by fitting the experimental data to the following function:

$$P_{\mathrm{tip}}(z) = \begin{cases} \dfrac{p_1}{z+p_2} + p_3 \ (\mathrm{z} \geq z_0) \\ p_4(z_0 - z)^{p_5} + \dfrac{p_1}{z+p_2} + p_3 \quad (\mathrm{z} \leq z_0) \end{cases} \tag{18}$$

with fitting parameters p_1, p_2, p_3, p_4, p_5, and z_0. z_0 corresponds to the position of the onset of the dissipation power at which the tip began touching the first water layer formed on the mica surface, and was found to be 0.07 nm. The fitted curve is shown in Fig. 3(a) with the original experimental data. The fitted curve was then converted to the damping curve using Eq. (14). The first, second, and third terms on the right side of Eq. (14) are presented in Fig. 3(b), respectively. The first term is identical with Fig. 3(a) in Ref. 12. The sum of the three terms is shown in Fig. 3(c). The damping obtained by Eq. (14) shows a more prominent rise at z_0 than the conversion only with the first tem in Eq. (14) (small amplitude limit).

We also subtracted the damping caused by the squeeze film damping of the mesoscopic tip, $\gamma_{\mathrm{film}}(z)$, from $\gamma_{\mathrm{tip}}(z)$, as presented in Ref. 12 using the following equation:

$$\gamma_{\mathrm{film}}(z) = \frac{6\pi\eta R^2}{z+h_0} + \gamma_{\mathrm{offset}}, \tag{19}$$

where h_0 is the difference between the mesoscopic and nanoscopic tips, and γ_{offset} is an offset. The fitting parameters were determined as $R = 24$ nm, $h_0 = 0.6$ nm, and $\gamma_{\mathrm{offset}} = -5$ nNs/m, respectively. $\gamma_{\mathrm{tip}}(z)$, $\gamma_{\mathrm{film}}(z)$, and $\gamma_{\mathrm{tip}}(z) - \gamma_{\mathrm{film}}(z)$, which correspond to the damping of the tip-sample system recovered from $P_{\mathrm{tip}}(z)$, the squeeze film damping of the mesoscopic tip (Eq. (19)), and the damping of the nanoscopic tip, respectively, are shown in Fig. 3(c). The damping onset observed when the tip started to interact with the adsorbed/first hydration layers is more precisely calculated from the experimental data, which is now more prominent than Fig. 3(b) in Ref. 12. It is suggested that the increased

damping might be because the viscosity of the adsorbed/first hydration layers is greater than that of the bulk water; however, the nonlinearity may also be a possible cause of the increased damping.[25]

In summary, we obtained the analytical equation to recover the damping from the experimental available dissipation power. The experimental curve of the damping with the colloidal probe was in good agreement with the theoretical damping curve. Moreover, we applied the equation to the dissipation power versus distance curve on the solution-mica interface, and showed that the damping of the adsorbed/first hydration layers was greater than that of the bulk solution. Based on the analytical equation presented here, FM-AFM is useful to quantitatively measure the viscosity of a nano-confined liquid with a high sensitivity as well as a high spatial resolution.

Authors deeply thank Prof. Dr. Peter Grütter for giving them the opportunity of conducting the present study. This work was supported by Grants-in-Aid for Scientific Research from the Ministry of Education, Culture, Sports, Science and Technology of Japan, and SENTAN Program of the Japan Science and Technology Agency.

[1]L. Bocquet and E. Charlaix, Chem. Soc. Rev. **39**, 1073 (2010).
[2]B. Bhushan, J. N. Israelachvili, and U. Landman, Nature **374**, 607 (1995).
[3]P. J. Feibelman, J. Phys. Chem. C **117**, 6088 (2013).
[4]H. Daiguji, Nat. Nanotechnol. **5**, 831 (2010).
[5]R. G. Horn, D. T. Smith, and W. Haller, Chem. Phys. Lett. **162**, 404 (1989).
[6]F. Liu, S. de Beer, D. van der Ende, and F. Mugele, Phys. Rev. E **87**, 062406 (2013).
[7]D. Ortiz-Young, H.-C. Chiu, S. Kim, K. Voitchovsky, and E. Riedo, Nat. Commun. **4**, 2482 (2013).
[8]S. H. Khan, E. L. Kramkowski, P. J. Ochs, D. M. Wilson, and P. M. Hoffmann, Appl. Phys. Lett. **104**, 023110 (2014).
[9]T. Fukuma, Y. Ueda, S. Yoshioka, and H. Asakawa, Phys. Rev. Lett. **104**, 016101 (2010).
[10]A. Labuda, K. Kobayashi, D. Kiracofe, K. Suzuki, P. H. Grutter, and H. Yamada, AIP Adv. **1**, 022136 (2011).
[11]K. Kobayashi, N. Oyabu, K. Kimura, S. Ido, K. Suzuki, T. Imai, K. Tagami, M. Tsukada, and H. Yamada, J. Chem. Phys. **138**, 184704 (2013).
[12]A. Labuda, K. Kobayashi, K. Suzuki, H. Yamada, and P. Grütter, Phys. Rev. Lett. **110**, 066102 (2013).
[13]F. J. Giessibl, Appl. Phys. Lett. **78**, 123 (2001).
[14]J. E. Sader and S. P. Jarvis, Appl. Phys. Lett. **84**, 1801 (2004).
[15]H.-J. Butt, B. Cappella, and M. Kappl, Surf. Sci. Rep. **59**, 1 (2005).
[16]J. P. Cleveland, B. Anczykowski, A. E. Schmid, and V. B. Elings, Appl. Phys. Lett. **72**, 2613 (1998).
[17]U. Dürig, Appl. Phys. A **72**, S43–S46 (2001).
[18]B. Gotsmann, C. Seidel, B. Anczykowski, and H. Fuchs, Phys. Rev. B **60**, 11051 (1999).
[19]J. E. Sader and Y. Sugimoto, Appl. Phys. Lett. **97**, 043502 (2010).
[20]K. Kobayashi, H. Yamada, and K. Matsushige, Rev. Sci. Instrum. **82**, 033702 (2011).
[21]C. P. Green and J. E. Sader, Phys. Fluids **17**, 073102 (2005).
[22]S. Basak, A. Raman, and S. V. Garimella, J. Appl. Phys. **99**, 114906 (2006).
[23]See supplementary material at http://dx.doi.org/10.1063/1.4903484 for interpretation of the frequency shift curve in Fig. 1(a) and validation of Eq. (14) regardless of the amplitude.
[24]H. Hölscher, B. Gotsmann, and A. Schirmeisen, Phys. Rev. B **68**, 153401 (2003).
[25]D. Kiracofe and A. Raman, Phys. Rev. B **86**, 205405 (2012).